

# Live Cell Imaging Reveals Structural Associations between the Actin and Microtubule Cytoskeleton in *Arabidopsis*

Arun Sampathkumar,<sup>a</sup> Jelmer J. Lindeboom,<sup>b</sup> Seth Debolt,<sup>c</sup> Ryan Gutierrez,<sup>d,e</sup> David W. Ehrhardt,<sup>d,e</sup> Tijs Ketelaar,<sup>b</sup> and Staffan Persson<sup>a,1</sup>

<sup>a</sup>Max Planck Institute of Molecular Plant Physiology, 14476 Potsdam, Germany

<sup>b</sup>Laboratory of Plant Cell Biology, Wageningen University, 6708 PB Wageningen, The Netherlands

<sup>c</sup>Department of Horticulture, University of Kentucky, Lexington, Kentucky 40546

<sup>d</sup>Department of Plant Biology, Carnegie Institution for Science, Stanford, California 94305

<sup>e</sup>Department of Biology, Stanford University, Stanford, California 94305

**In eukaryotic cells, the actin and microtubule (MT) cytoskeletal networks are dynamic structures that organize intracellular processes and facilitate their rapid reorganization. In plant cells, actin filaments (AFs) and MTs are essential for cell growth and morphogenesis. However, dynamic interactions between these two essential components in live cells have not been explored. Here, we use spinning-disc confocal microscopy to dissect interaction and cooperation between cortical AFs and MTs in *Arabidopsis thaliana*, utilizing fluorescent reporter constructs for both components. Quantitative analyses revealed altered AF dynamics associated with the positions and orientations of cortical MTs. Reorganization and reassembly of the AF array was dependent on the MTs following drug-induced depolymerization, whereby short AFs initially appeared colocalized with MTs, and displayed motility along MTs. We also observed that light-induced reorganization of MTs occurred in concert with changes in AF behavior. Our results indicate dynamic interaction between the cortical actin and MT cytoskeletons in interphase plant cells.**

## INTRODUCTION

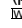
The cytoskeleton supports many fundamental cellular processes, including morphogenesis, cell division, and vesicle trafficking (Goode et al., 2000; Fu et al., 2005; Collings, 2008; Gutierrez et al., 2009; Petrásek and Schwarzerová, 2009; Szymanski, 2009). The actin filaments (AFs) and microtubules (MTs) were formerly viewed as two distinct networks with separate functions, but were found to cooperate in yeast (*Saccharomyces cerevisiae*) and animal cells (Goode et al., 2000). For example, coalignment of AFs and MTs was observed in *Taricha granulosa* (newt) lung epithelial cells (Salmon et al., 2002), and MTs were transported in association with AFs to sites of induced wounding in *Xenopus laevis* oocytes (Mandato and Bement, 2003). Whereas AFs and MTs are common to eukaryotic organisms, structural and functional differences are evident in plant species; perhaps due to the presence of a rigid cell wall and a large central vacuole, and also due to the absence of the cytoskeleton-organizing centers referred to as centrosomes in animal cells and as spindle pole bodies in yeast cells (Ehrhardt and Shaw, 2006).

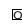
Reports of AF and MT associations in plants are scarce, but are supported by imaging of fixed tissues, pharmacological studies, and the existence of common binding partners (Collings, 2008). In fixed tissues, fine transverse AFs have been observed as an ordered array, reminiscent of the transverse arrangements of MTs (Collings and Wasteneys, 2005), and AFs and MTs have been observed to coalign (Traas et al., 1987; Blancaflor, 2000; Collings and Wasteneys, 2005; Barton and Overall, 2010). MT depolymerization resulted in partial loss of the fine transversely oriented cortical AFs in *Arabidopsis thaliana* and carrot (*Daucus carota*) cells, leading to the proposal that associations between the AFs and MTs may occur (Traas et al., 1987; Collings and Wasteneys, 2005). In addition, environmental or developmental cues have been documented to induce changes in MTs and AFs, hinting at coordinate action. For example, reorientation of the MT array was concurrent with changes in AF organization in tracheary elements of developing *Zinnia elegans* cells (Kobayashi et al., 1988), and disruption of the AFs impaired MT reorganization, an effect that also was observed in azuki bean (*Vigna angularis*) cells (Takesue and Shibaoka, 1998).

The use of electron and confocal microscopy has allowed for a basic understanding of the behavior of the individual cytoskeleton components (Traas et al., 1987; Shaw et al., 2003; Sheahan et al., 2004; Staiger et al., 2009). Because the AFs and MTs are highly dynamic (Shaw et al., 2003; Staiger et al., 2009), a plausible scenario is that interactions occur only briefly, which would make them challenging to capture in static images by electron microscopy. Monitoring both components in real time using

<sup>1</sup> Address correspondence to Persson@mpimp-golm.mpg.de.

The author responsible for distribution of materials integral to the findings presented in this article in accordance with the policy described in the Instructions for Authors (www.plantcell.org) is: Staffan Persson (persson@mpimp-golm.mpg.de).

 Online version contains Web-only data.

 Open Access articles can be viewed online without a subscription. www.plantcell.org/cgi/doi/10.1105/tpc.111.087940

stably transformed cells with dual-labeled reporter constructs may provide a powerful tool for revealing coordinate behavior and elucidating the underlying principles. Only two previous reports, one focusing on trichomes (Saedler et al., 2004) and the other on root hairs (Timmers et al., 2007), have used dual-labeled probes for AFs and MTs in plants, but evidence for or against heterotypic interaction remains needed.

We have investigated coordinated AF and MT activities, using spinning disc confocal microscopy of dual-labeled lines, coupled with pharmacological studies. We deduce quantitatively that AFs and MTs interact dynamically, and that the AFs depend on the MTs to recover following drug-induced depolymerization events and for reorganization following light stimulus.

## RESULTS

### Stabilization of the Actin Cytoskeleton Leads to Aberrant MT Organization

Several studies have assessed MT behavior after AF disruption via pharmacological agents such as latrunculinB (latB) and cytochalasinB (Collings, 2008). Here, we tested whether a more stable actin configuration had an impact on the organization of MTs using the drug jasplakinolide (Bubb et al., 1994). Because jasplakinolide has not been extensively employed in plant cell biology, we first grew *Arabidopsis* seedlings on different concentrations of the drug and assessed the impact on growth (see Supplemental Figures 1A to 1E online). From these experiments, and subsequent experiments using seedlings expressing green fluorescent protein (GFP):F-actin binding domain of fimbrin1 (FABD) (Ketelaar et al., 2004), we determined that 5  $\mu$ M was a suitable concentration for short-term jasplakinolide treatments. Short-term treatment of 5-d-old seedlings with jasplakinolide (5  $\mu$ M for 3 h) revealed that actin bundles and filaments became fragmented, rigid, and less dynamic in hypocotyl cells (Figures 1A and 1B; see Supplemental Movie 1 online). To investigate whether this behavior was reversible, we performed washout experiments for a period of 48 h, and we observed that the AFs recovered (see Supplemental Figure 1F online). To assess the impact of this treatment on the MTs, we exposed 5-d-old seedlings expressing mCherry: $\alpha$ -tubulin 5 isoform (TUA5) (Gutierrez et al., 2009) to the same treatment conditions. Interestingly, MT orientation was less ordered after short-term treatment of jasplakinolide compared with controls (Figures 1C and 1D). As previously observed (Paredes et al., 2006), cortical MTs in elongating cells were transversely or obliquely oriented to the cell axis in arrays with marked parallel ordering (Figures 1C and 1E). Treatment with jasplakinolide caused a striking loss of array order (Figures 1D and 1E). To check whether MT dynamics were influenced by jasplakinolide treatment, we measured the growth ( $v_g$ ) and shrinkage velocities ( $v_s$ ) of the plus end of single MTs. No significant differences were found between the jasplakinolide- and mock-treated cells (Figure 1F).

Because the mode of action of jasplakinolide as an actin-stabilizing drug in plant cells was not established prior to this

study, it was important to test whether the drug cross-reacted with MTs, thereby disturbing MT organization. To test this hypothesis, we generated *Arabidopsis* plants coexpressing mCherry:TUA5 and GFP:FABD. Dual-labeled 5-d-old seedlings were treated with 1  $\mu$ M latB for 6 h, and 5  $\mu$ M jasplakinolide was added for an additional 6 h. As expected, the latB treatment completely removed the actin cytoskeleton and only free GFP:FABD was observed (see Supplemental Figure 1G online). In the absence of AFs, the MTs in jasplakinolide-treated cells remained arranged as observed in control-treated seedlings (see Supplemental Figures 1G and 1H online), i.e., the latB/jasplakinolide-treated seedlings displayed MTs with parallel orientation (see Supplemental Figure 1G online). Thus, the effect of jasplakinolide on cortical MT organization was dependent on actin assembly and was not due to action of the drug on a second target.

To assess the organization of the fragmented actin cytoskeleton relative to MTs, we treated 5-d-old GFP:FABD and mCherry:TUA5 dual-labeled seedlings with jasplakinolide. Interestingly, static AFs, which were present throughout the cortical focal plane, appeared to align with MTs (Figure 1G; see Supplemental Movie 2 online). In addition, a fraction of small actin fragments was observed to align with and move along paths defined by MTs (see Supplemental Movie 2 online).

Together, these results suggested the possibility of crosstalk between the actin and MT cytoskeletons in that alteration of actin assembly or turnover, as perturbed by jasplakinolide, was correlated with loss of MT organization, and stabilized AFs were found to align with and move along MTs.

### Cortical AFs Transiently Coalignment with MTs

The alignment between fragmented AFs and MTs in the jasplakinolide-treated cells prompted us to investigate whether the two cytoskeletal structures also interact under normal conditions. Confocal observation of dual-labeled hypocotyl cells of 3-d-old etiolated seedlings revealed numerous sites where cortical AFs and MTs were colocalized and coaligned (Figures 2A to 2C; see Supplemental Movies 3 and 4 online). Coalignment between the MTs and AFs was observed mainly between transversely or obliquely oriented AFs and MTs at the cell cortex; however, in some instances, we also observed alignment between longitudinal cortical actin bundles and MTs. The AFs emerged from lower focal planes or moved across the cortical optical plane, and aligned with MTs (Figures 2D and 2E; see Supplemental Movies 3 and 4 online). Straightening and bending events of cortical AFs, as reported by Staiger et al. (2009), were also observed to coalign with MTs in some cases (Figure 2E; see Supplemental Movie 4 online).

Some degree of colocalization and coalignment of the two labeled cytoskeletal structures would be expected by chance alone if the two systems were independent. We analyzed the dynamics of coalignment to determine if it was non-random. We observed that sections of dynamic AFs that aligned with MTs were frequently stabilized in this configuration over short periods of time (Figures 2D and 2E). We refer to these stabilized AF configurations as AF pauses. We surveyed AF pausing that

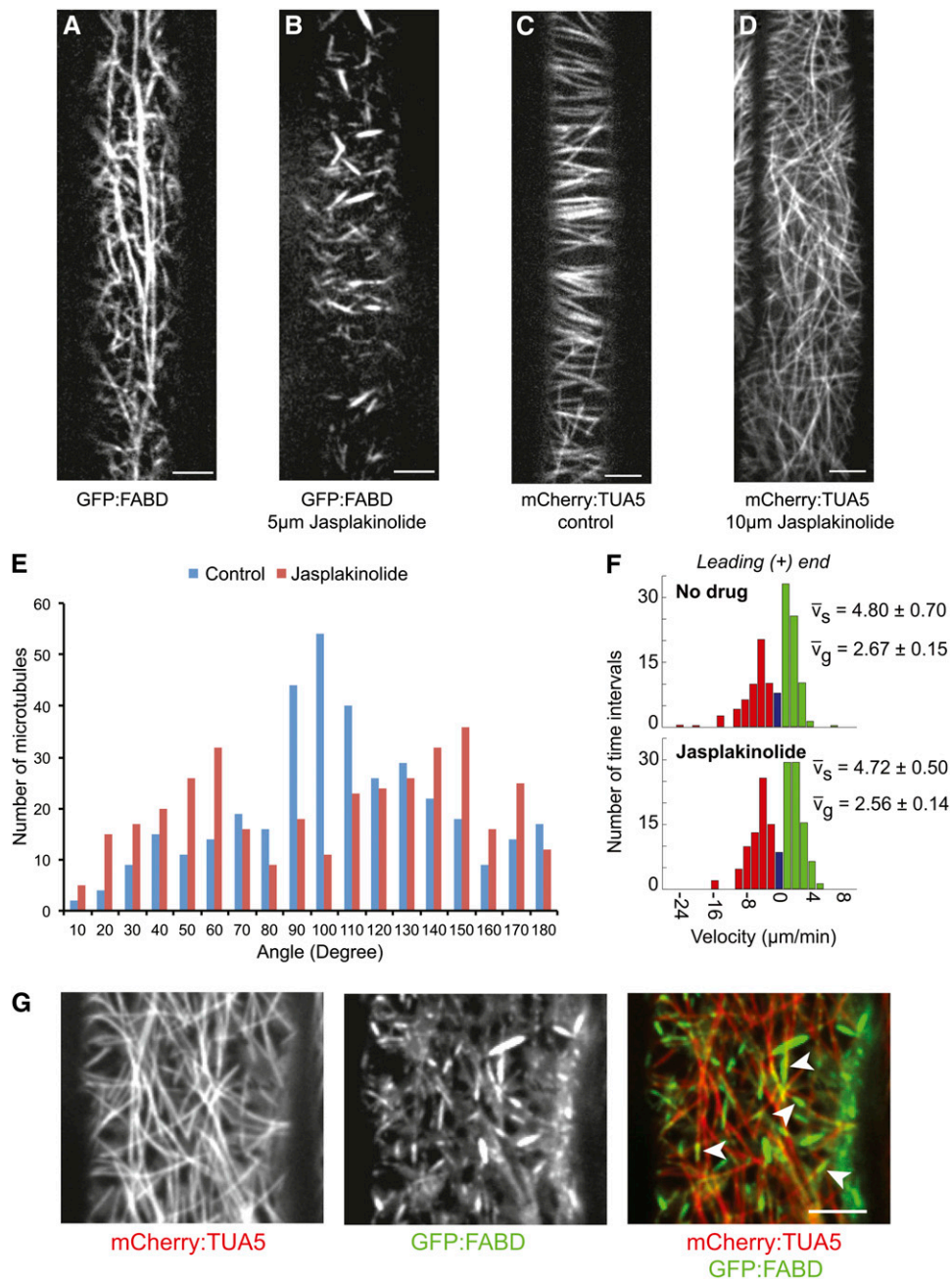


**Figure 1.** Jasplakinolide Affects MT Orientation through Stabilization of the Actin Cytoskeleton.

**(A)** and **(B)** Organization of the actin cytoskeleton in mock-treated **(A)** and jasplakinolide-treated **(B)** hypocotyl cells of GFP:FABD-expressing 5-d-old etiolated seedlings.

**(C)** and **(D)** MT organization in control **(C)** and jasplakinolide-treated (5  $\mu$ M for 3 h **[D]**) hypocotyl cells of YFP:TUA5-expressing 5-d-old etiolated seedlings.

**(E)** Histogram documenting distribution of MT angles with regard to the growth axis.

**(F)**  $v_g$  and  $v_s$  were measured for the leading ends of single MTs ( $\pm$  SE). Histograms are presented showing shrinkage (red), growth (green), and pause (blue).

**(G)** Actin fragments reside in transient coincidence with cortical MTs after jasplakinolide treatment (5  $\mu$ M for 6 h). White arrowheads indicate actin fragments aligned with MTs. Scale bars = 5  $\mu$ m.

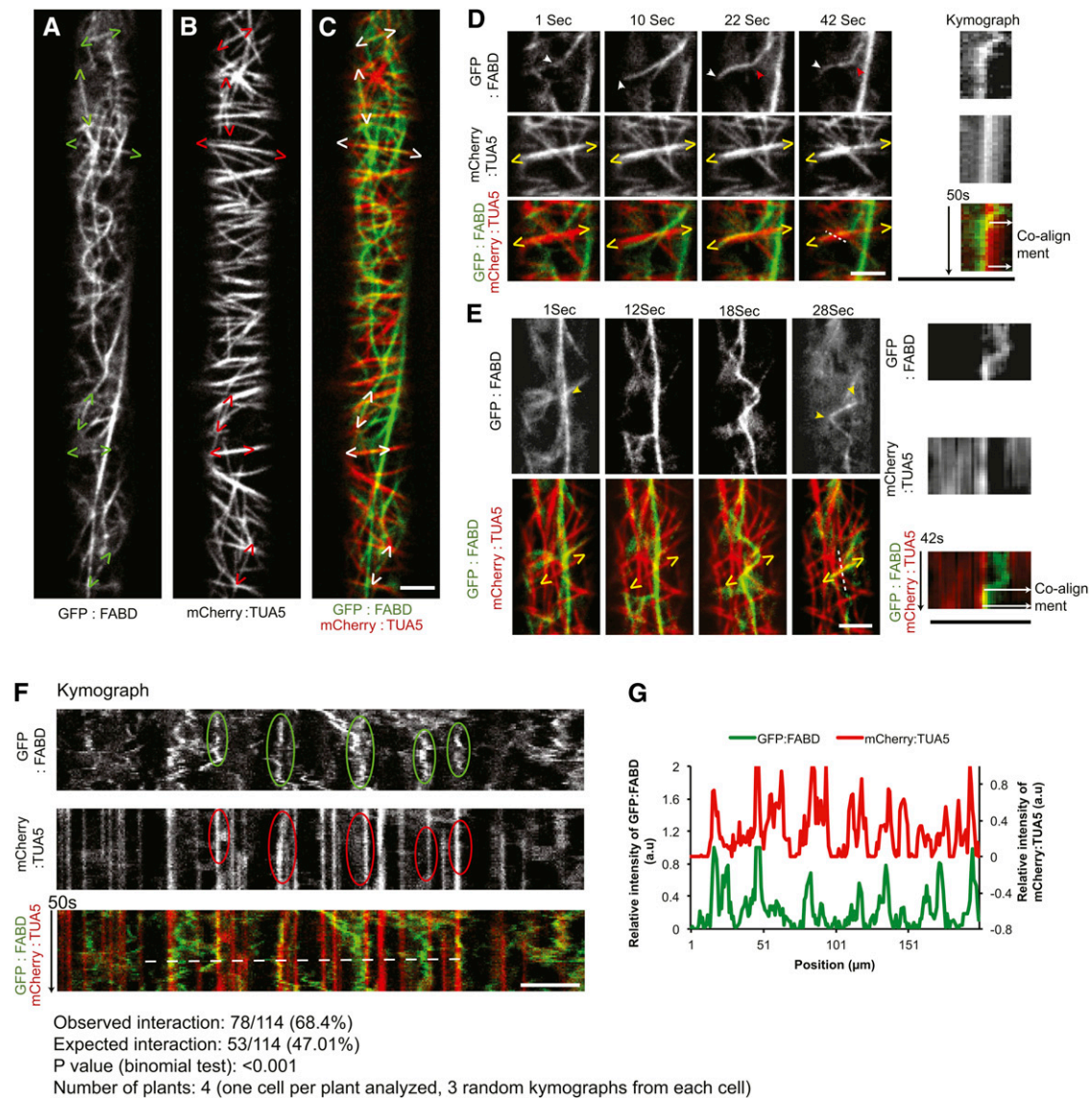


**Figure 2.** Coalignment between Cortical AFs and MTs in *Arabidopsis* Hypocotyl Cells.

**(A) to (C)** Dual-labeled GFP:FABD **(A)** and mCherry:TUA5 **(B)**, and merge of A and B **(C)**, observed in hypocotyl cells of 3-d-old etiolated seedlings. Carets enclose regions of co-occurrence of the two channels.

**(D)** Selected frames from a time series of a GFP:FABD and mCherry:TUA5 dual-labeled line. Red arrowheads indicate regions where AFs appear static after MT alignment. White arrowhead indicates that AFs emerge from a lower focal plane, and yellow carets enclose the region of MT and AF coalignment. The far right panel shows a kymograph corresponding to the dashed white line, with time on the vertical axis.

**(E)** AF bending and straightening events facilitate alignment between AFs and MTs. Yellow arrowheads indicate the region of the AF that exhibits bending, and yellow carets enclose the region of the coaligned MT and AF. The far right panel shows a kymograph corresponding to the white dashed line, with time on the vertical axis.

**(F)** Kymograph covering the entire cell length showing multiple static AF events (green enclosure) that coincided with MTs (red enclosure). Only AFs that were static for more than 30 s were considered.

**(G)** A fluorescence intensity plot of a transect of the kymograph shown in **(F)** [white dashed line]. a.u., arbitrary units. Scale bars = 5  $\mu\text{m}$ .

occurred for 30 s or longer using linear transects and kymograph analysis along the entire cell length and we found that the majority of AF pauses coincided with MTs. Of the 114 pause events observed in four cells, 78 (or 68.4%) coincided with MTs (Figures 2F and 2G), which is significantly higher than the 53 events ex-

pected by chance based on MT signal coverage in the images ( $P < 0.001$ , binomial test, see Methods). The majority of the nonpausing AFs in the kymograph did not align with the MTs. Hence, changes in AF dynamics were associated with MT juxtaposition.

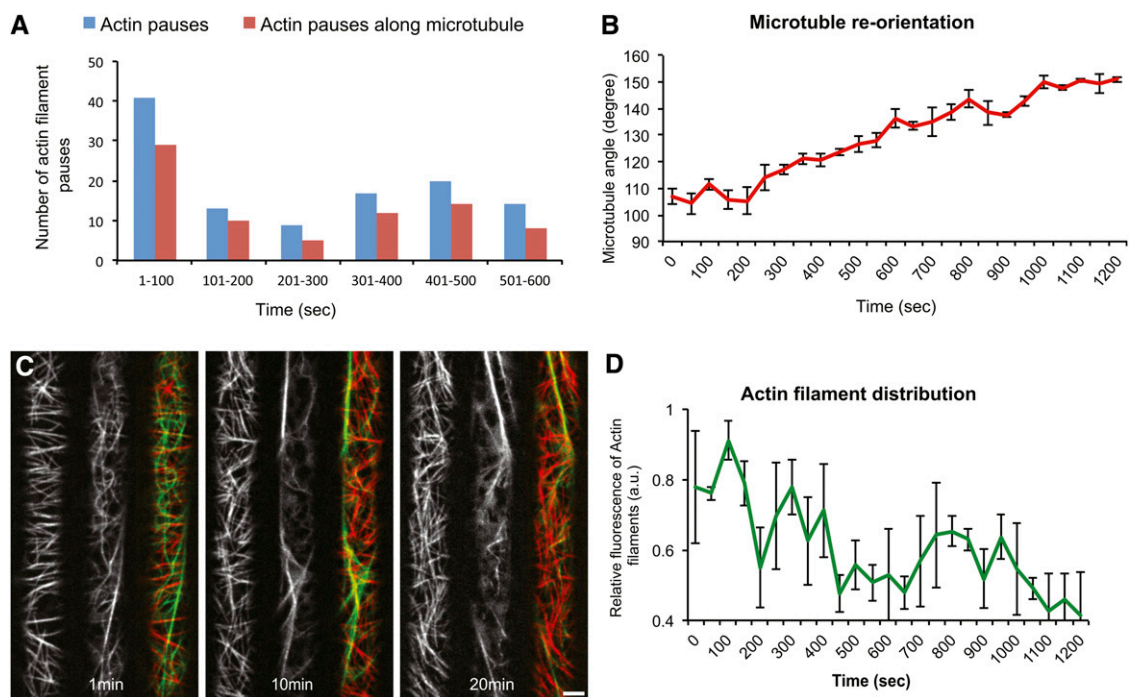


**Figure 3.** Light-Induced Rearrangements of the Cytoskeleton.

(A) Histogram showing actin–MT interaction over time ( $n = 4$  cells).

(B) Changes in average MT angle over time during the process of imaging ( $n = 3$  cells). Error bars represent SE.

(C) Selected frames from a time series of a GFP:FABD and mCherry:TUA5 dual-labeled line at the hypocotyl cell cortex in etiolated 3-d-old seedlings after light exposure.

(D) Changes in relative fluorescence intensity of AFs over time ( $n = 3$  cells). Error bars represent SE. a.u., arbitrary units. Scale bars = 5  $\mu\text{m}$ .

### Coordinated Changes to AFs and MT Organization upon Light Induction

We observed that 35% of the AF pausing events (see Figure 2) occurred during the first 50 s of imaging (Figure 3A; see Supplemental Figure 2A online). The other pausing events were observed during the remaining 10 min of imaging. Thus, observation of pausing was significantly biased to the beginning of the observation interval, indicating that the act of observation may influence the frequency of pausing. This was reminiscent of previous observations that transversely oriented MTs in etiolated hypocotyl cells rearrange in response to light during observation (Ueda and Matsuyama, 2000; Paredez et al., 2006). However, comparable analyses for light-induced changes in AFs are lacking. Consistent with previous studies, we confirmed that MTs rearranged from a largely transverse orientation to a more oblique array under our imaging conditions (Figures 3B and 3C). We then observed the organization and behavior of the AFs and MTs in 3-d-old dual-labeled dark-grown hypocotyls (Figure 3C; see Supplemental Movie 5 online). Intriguingly, time-series images revealed that the cortical and mainly transversely oriented AFs became progressively less prevalent during imaging (Figures 3C and 3D). The altered behavior of AF distribution at the cell cortex occurred in tandem with the light-induced rearrangement of the MT array (Figures 3B and 3D). To investigate whether the changes in behavior of AFs were influenced by the MT cytoskel-

eton, we treated seedlings expressing mCherry:TUA5 with 20  $\mu\text{M}$  oryzalin (an MT-depolymerizing drug) overnight to ensure complete depletion of MTs (see Supplemental Figure 2B online). The spatial distribution of the AF signal remained nearly constant throughout the imaging process in the absence of the MT cytoskeleton (see Supplemental Figures 2C and 2D online). These results indicate that the organization of MTs may, directly or indirectly, influence the distribution of AFs at the cortex.

### AFs Recover along MTs following Washout of LatB

To investigate further the dynamic interactions between AFs and MTs, we assessed reassembly behavior of both structures after depolymerization. We treated 3-d-old dual-labeled GFP:FABD and mCherry:TUA5 seedlings with latB overnight, and then allowed for actin recovery after washout of the drug. The overnight latB treatment resulted in complete removal of the labeled actin cytoskeleton in hypocotyl cells. At about 3 h after latB washout, short fragments of actin label began to appear at the cell cortex (Figure 4A; see Supplemental Movie 6 online). These nascent foci of actin label appeared in linear arrays that coincided with MTs in image overlays and line scan analyses (Figures 4A and 4B; see Supplemental Movie 6 online). These observations indicate that new actin polymerization can be initiated at positions coinciding with cortical MTs.

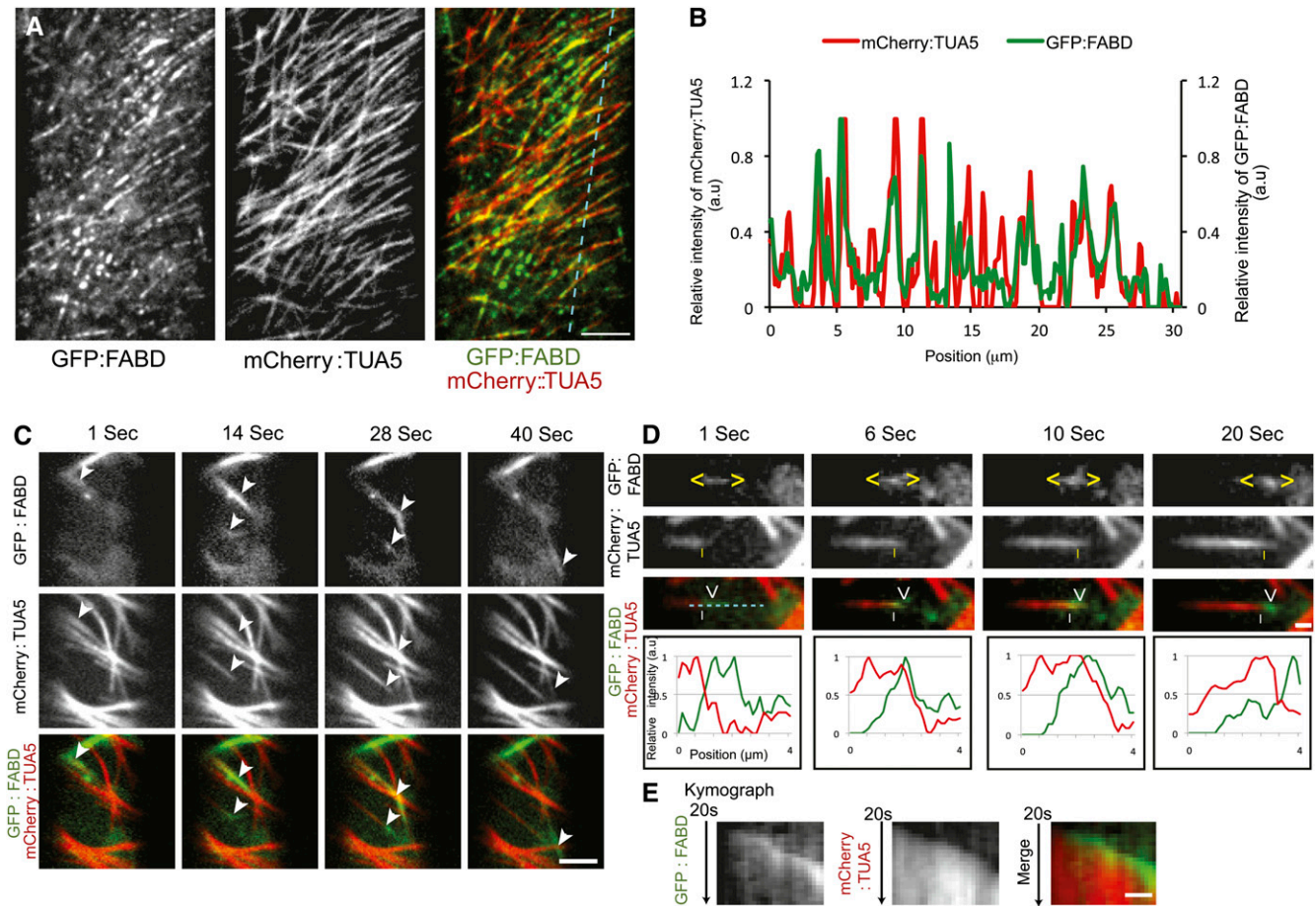


**Figure 4.** Recovery of the Actin Cytoskeleton following latB Treatment and Washout Requires MTs.

**(A)** Newly formed AFs coincide with MTs 3 h after latB washout.

**(B)** Fluorescence intensity plot of the GFP:FABD and mCherry:TUA5 signals across a transect of an elongating hypocotyl cell (cyan line shown in **[A]**). a.u., arbitrary units.

**(C)** Selected frames from a time series of a GFP:FABD and mCherry:TUA5 dual-labeled line at the hypocotyl cell cortex in etiolated 3-d-old seedlings 5 h after latB washout. White arrowheads indicate the movement of small AF fragments along MTs. Scale bar = 5  $\mu\text{m}$ .

**(D)** Selected frames from a time series of a GFP:FABD and mCherry:TUA5 dual-labeled line at the cell cortex 5 h after latB washout. Yellow carets enclose small actin structures that move along the MT plus end (yellow vertical line). Bottom panel, fluorescence intensity plot of the GFP:FABD and mCherry:TUA5 signals along the cyan line in top panel.

**(E)** Kymograph of the cyan line in image **(D)**. Scale bars = 1  $\mu\text{m}$ .

The labeled AFs increased in size during recovery from an average of  $0.85 \pm 0.30 \mu\text{m}$  (3 h after latB washout) to  $2.15 \pm 0.75 \mu\text{m}$  and  $4.18 \pm 2.03 \mu\text{m}$ , after 5 and 8 h of recovery, respectively ( $n = 100$ , three cells from three seedlings). Intriguingly, 5 h after latB washout, reformed AF fragments were observed traveling along cortical MTs with varying velocities, i.e., 7.4 to 17.3  $\mu\text{m}/\text{min}$  ( $n = 37$ ; Figure 4C; see Supplemental Movie 7 online). From time series taken from three cells, we observed 12 incidences of reformed actin fragments that migrated together with dynamic MT plus ends (Figures 4C to 4E; see Supplemental Movie 8 online). It is important to note that the actin cytoskeleton had almost completely recovered 24 h after latB washout, indicating that the pharmacological effects were reversible (Figure 5B; see

Supplemental Movie 9 online). Together, these results corroborate interaction and coalignment between AFs and MTs *in vivo*.

The observed re-emergence of AFs along MTs suggests that AF polymerization can occur at MT sites in *Arabidopsis* cells. We investigated time series images of mCherry:TUA5 and GFP:FABD dual-labeled lines, and observed instances of polymerization of new AFs emanating from existing actin bundles that were colocalized with MTs (see Supplemental Figure 2E and Supplemental Movie 10 online). However, reliable quantitative analysis of such events was not possible due to the highly crowded and dynamic nature of the cytoskeleton arrays under steady state conditions.

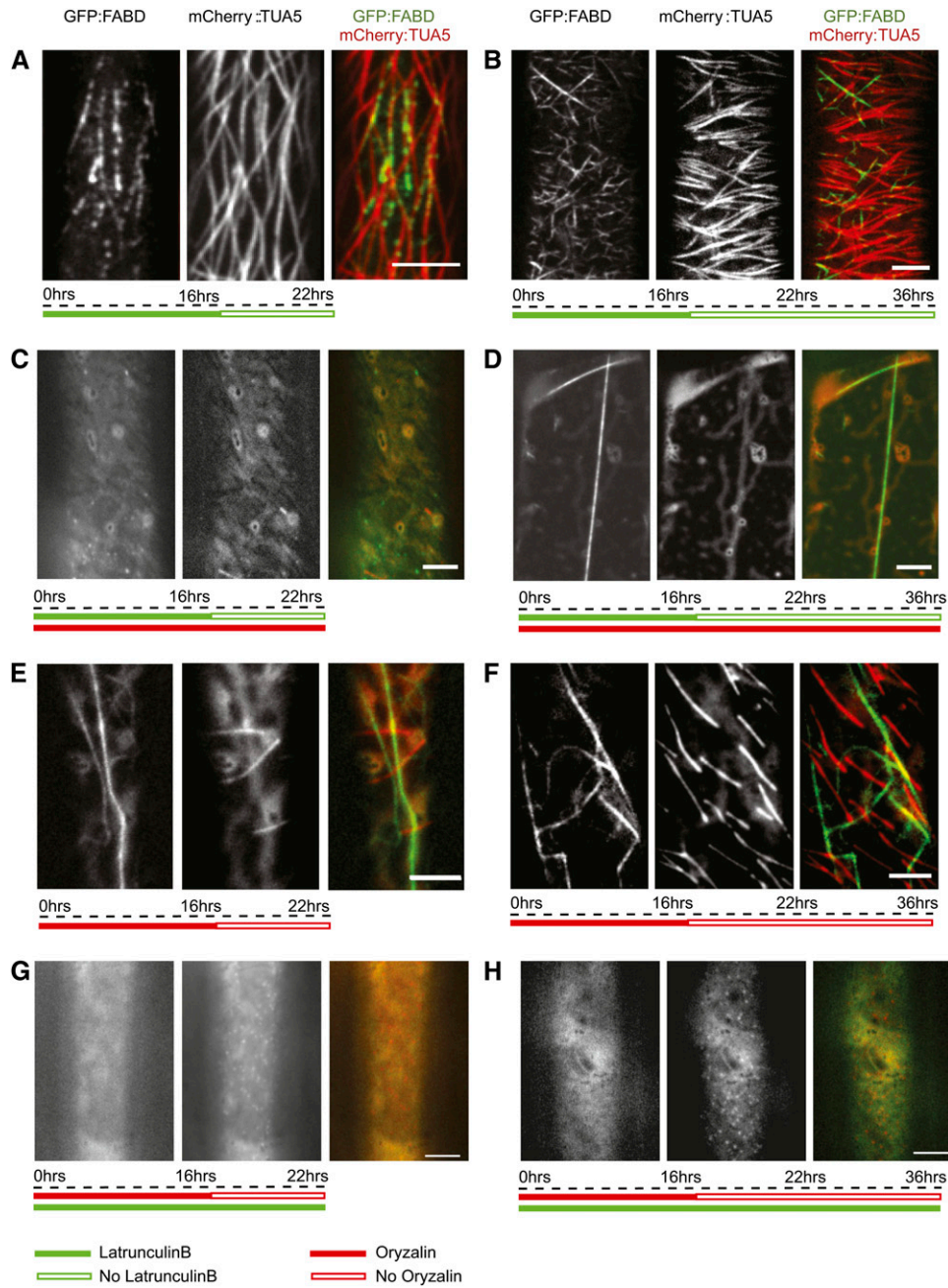


**Figure 5.** Mutual Dependence of the Actin and MT Cytoskeleton Assayed by Recovery after Depolymerization.

**(A)** and **(B)** One micromolar latB treatment of GFP:FABD and mCherry:TUA5 dual labeled etiolated 3-d-old seedlings for 16 h followed by washout of latB and recovery of the actin cytoskeleton for 6 h **(A)** and 20 h **(B)**.

**(C)** and **(D)** One micromolar latB and 20  $\mu$ M oryzalin treatment for 16 h followed by washout of latB and recovery of the actin cytoskeleton for 5 h **(C)** and 20 h **(D)**.

**(E)** and **(F)** Oryzalin treatment of GFP:FABD and mCherry:TUA5 dual labeled lines for 16 h followed by washout of oryzalin and recovery of MTs for 5 h **(E)** and 20 h **(F)**.

**(G)** and **(H)** LatB and oryzalin treatment for 16 h followed by washout of oryzalin and recovery of MTs for 5 h **(G)** and 20 h **(H)**. Scale bars = 5  $\mu$ m.

### Mutual Dependence of the Actin and MT Cytoskeleton Assayed by Recovery after Depolymerization

The experiments above present evidence for actin regeneration along MTs. To test if the MTs are needed for AF recovery, we depolymerized both cytoskeleton components by treating them with latB and oryzalin overnight. We then washed out latB, but maintained the oryzalin treatment. After 6 h of recovery in the presence of oryzalin, only diffuse GFP:FABD signal and sparse punctae of actin label were observed. These fragments were neither fixed in position like the nascent punctae in cells with intact MTs, nor did they show rapid long range movement consistent with cytosolic streaming; rather, they displayed limited and erratic movement (Figure 5C; see Supplemental Movie 11 online) consistent with Brownian motion. After 20 h of recovery, most cells showed a similar punctate pattern of actin foci as observed after 6 h. However, we also observed single straight actin rods, or bundles, which were stationary over the time of observation (Figure 5D; see Supplemental Movie 12 online). Thus, recovery of actin structures labeled by GFP:FABD was sensitive to oryzalin treatment, suggesting that MTs or an MT-dependent cell function is required for reassembly of the actin cytoskeleton after depolymerization.

To investigate the influence of AFs on MT recovery, we also performed oryzalin washout experiments in the absence or presence of the actin cytoskeleton. In the absence of latB, MTs began to recover 5 h after oryzalin washout (Figure 5E; see Supplemental Movie 13 online), and tread-milling MTs were present throughout the cell cortex after 20 h (Figure 5F; see Supplemental Movie 14 online). However, in cells pretreated with latB, only small punctae of MT label were visible 6 h after oryzalin washout (Figure 5G; see Supplemental Movie 15 online). In addition, apart from the punctate patterns of fluorescence, the majority of the cells lacked conspicuous MT polymers 20 h after washout in the absence of the actin cytoskeleton (Figure 5H; see Supplemental Movie 16 online).

It is important to note that cells treated overnight with both cytoskeleton inhibitors for up to 16 h could recover 48 h after transfer to media without the drugs (see Supplemental Figure 3A and Supplemental Movie 17 online). Although similar recovery analysis of seedlings in long-term treatments (20 h with an additional 16-h treatment) did not recover, seedlings that underwent 6-h treatments with either one of the inhibitors after the overnight treatment with both inhibitors were able to recover (see Supplemental Figures 3B and 3C, and Supplemental Movies 18 and 19 online). Taken together, these observations indicate that MT and AF recovery following inhibitor treatments depends on the presence or function of the other cytoskeleton component.

## DISCUSSION

Dynamic interactions between AFs and MTs have been reported in animal systems (Goode et al., 2000). In plants, proximity of AFs and MTs has been observed only in fixed tissues (Traas et al., 1987; Blancaflor, 2000; Collings and Wasteneys, 2005; Barton and Overall, 2010). We present evidence based on live-cell imaging that cortical AFs and MTs interact and that cortical MT or MT function is required for re-establishing the cortical actin

cytoskeleton after disassembly. Previous studies speculated that MTs could influence the orientation of newly formed AFs (Hussey et al., 1998), an idea consistent with our observations that emerging actin fragments coincided with, and traveled along, MTs during reassembly.

Several studies have shown that perturbations of one cytoskeletal component can change the organization of the other (for review, see Collings, 2008). For example, disruption of the AF array using cytochalasinD affected MT organization in developing *Zinnia elegans* tracheary cells (Kobayashi et al., 1988). Jasplakinolide has previously been reported to cause delayed self-incompatibility-induced MT depolymerization in pollen tubes of *Papaver rhoeas* (Poulter et al., 2008). Our observations show that jasplakinolide induced changes in F-actin assembly and turnover, and affected the orientation and parallel ordering of MTs in etiolated hypocotyl cells. Whereas the mechanism of jasplakinolide action on MT organization is not known, one possible class of mechanism is steric interference by stabilized AFs, which could inhibit MT–MT interactions (Dixit and Cyr, 2004; Ehrhardt and Shaw, 2006), MT membrane attachment (Ehrhardt and Shaw, 2006; Ambrose and Wasteneys, 2008), or recruitment and function of MT-associated nucleation complexes (Murata et al., 2005; Nakamura et al., 2010).

Studies using fixed plant tissues have reported that AFs and MTs sometimes appear in close proximity to each other; however, no quantitative measurements have been reported. Cortical AFs in *Arabidopsis* are highly dynamic structures that exhibit rapid growth and severing (Staiger et al., 2009). During these events, they also display deformations described as buckling and straightening (Staiger et al., 2009). Transient coalignment between these rapidly reorganizing AFs and MTs may be observed in fixed tissue, but the stability of this alignment cannot be evaluated easily. Using live-cell imaging combined with image analysis, we were able to quantitatively study this transient coalignment. This analysis showed that pauses in AFs are more frequent in proximity to MTs, suggesting interaction between AFs and MTs or molecules at the cell cortex organized by MTs.

To study these interactions further, we made use of a physiologically driven change in cytoskeletal organization (Ueda and Matsuyama, 2000; Chan et al., 2007). In agreement with previous studies (Paredes et al., 2006), we observed that the transverse MT organization gradually changes to a longitudinal organization upon light exposure and resulted in a reduction of coalignment between AFs and MTs. These changes were accompanied by a decrease in cortical AF density. Thus, in addition to the light-induced MT reorganization showed previously (Paredes et al., 2006; Chan et al., 2007), we showed that the actin cytoskeleton was also affected. Whereas reorientation of cortical MTs has been shown to drive reorientation of cellulose synthase trajectories (Chan et al., 2010), it remains to be determined what functions associated with cell growth might be altered by the observed changes in actin distribution.

The light-induced changes in actin distribution appeared to be dependent on the presence of an intact MT cytoskeleton. Whereas this could signify a direct relationship between the two cytoskeletal arrays, it is important to note that removal of the MTs also affects cell growth (see Supplemental Figure 1D online; Baskin et al., 1994). Therefore, it is difficult to deduce whether the



MTs orchestrate the changes of the AF array directly, or whether these changes are due to alterations in growth. In plant cells, the photoreceptor proteins cryptochrome (Chaves et al., 2011) and/or phototropin (Christie, 2007) are involved in blue light-induced inhibition of hypocotyl cell elongation, and could be involved in triggering the orchestrated changes of the cytoskeleton components. The proteins that communicate light perception from plant cell photoreceptors to MT rearrangements have yet to be identified, but studies of chloroplast movements in *Arabidopsis* have revealed targets of blue light photoreceptors associated with the actin cytoskeleton, including THRUMIN1, a protein that mediates movement of chloroplasts via changes in actin bundling in response to blue light (Whippo et al., 2011), and KAC1/2, newly discovered kinesins that may interact with AFs rather than MTs (Suetsugu et al., 2010). Identification of additional proteins that are involved in transduction of light signals to the cytoskeleton is required for understanding how signaling to both cytoskeletons may be coordinated.

Pharmacological studies have increased our understanding of interactions and crosstalk between the two cytoskeleton components (Collings, 2008). AF recovery after microinjection of a pollen-specific actin depolymerization factor in *Tradescantia blossfeldiana* stamen hairs showed that AFs reappeared as transverse arrays, similar to the orientation of MT arrays rather than the longitudinal AF arrays found in untreated cells (Hussey et al., 1998). Similarly, injection of an antiserum against an actin bundling protein resulted in the dispersal of thick actin bundles into fine AFs at the same cortical plane as the MTs in root hair cells of *Hydrocharis bubia* (Tominaga et al., 2000). The authors speculated that MTs could influence the orientation of newly formed AFs. Our observations of AFs after latB washout provide direct evidence of AF polymerization along cortical MTs and indicate that cortical MTs may play a role in positioning actin nucleation.

Supporting the possibility that cortical MTs may position actin nucleation, Deeks et al. (2010) reported that the *Arabidopsis* FORMIN4 colocalized with MTs and could interact with the actin and MT cytoskeleton through a MT binding domain. Similarly, another formin, *Arabidopsis* FORMIN14, was found to interact with MTs and AFs during the process of cell division (Li et al., 2010). Such proteins could position actin nucleation at MTs. Some MT plus end tracking proteins associate with formins in yeast and animals (Wen et al., 2004; Martin and Chang, 2005), and MT plus ends have also been shown to play a role in deploying regulatory factors for actin nucleation in fission yeast and animal tissue culture cells (reviewed in Basu and Chang, 2007). It remains to be determined if plus end tracking proteins also interact with formins or other actin nucleation factors in plant cells. Whereas new actin growth is easily observed following latB washout, it has proved challenging to quantify locations of new AF growth under normal conditions of cell growth, in large part due to the density and dynamics of the cortical actin cytoskeleton. It is anticipated that future studies in which actin nucleating proteins can be observed in concert with labeled AF will help to address these challenges, much as observation of MT nucleation complexes has improved analysis of MT nucleation (Nakamura et al., 2010).

One of the more intriguing observations in this study is the movement of actin fragments along cortical MTs in jasplakinolide-treated cells and during recovery from latB treatment. Kinesin

motors, such as the cotton (*Gossypium hirsutum*) kinesins KCH1 and KCH2, have been described that localize to MTs and to fine AFs, possibly through the presence of a unique calponin homology domain (Preuss et al., 2004; Xu et al., 2009). Perhaps a similar mechanism is acting during the transport of the newly formed AFs along the MTs observed in our study.

AF recovery after latB washout revealed actin fragments colocalizing with MTs, indicating that MTs could serve as a scaffold for actin nucleation. The mechanism by which MT recovery is dependent on the actin cytoskeleton is less clear. AFs, along with actin binding proteins, may be required for the early stages of cortical MT array establishments. On the other hand, and unlike the AF recovery experiments, the recovery of MTs after oryzalin washout did not reveal any physical association between AFs and MTs. Further, live cell imaging studies of MT nucleation complexes did not reveal any changes in cortical association of the complexes, or any difference in MT nucleation dynamics, after AF depolymerization (Nakamura et al., 2010). Whereas this does not rule out a direct interaction between the AFs and re-emerging MTs after the oryzalin washout, it may suggest that other mechanisms are responsible for our observation. One plausible explanation is that the washout of oryzalin may be dependent on actin-based cytoplasmic streaming. Washout of oryzalin, which has a high affinity for free tubulin dimers (Strachen and Hess, 1983; Morejohn et al., 1987), is heavily dependent on the rate of transport of already internalized oryzalin molecules from the cytoplasm to sites at the plasma membrane to exit the cell. The presence of a cuticle could further act as a barrier and reduce efflux of oryzalin from hypocotyl cells. Therefore, the depolymerization of AFs could drastically decrease the speed at which oryzalin molecules are being removed from the cytosol.

In summary, we show that cortical AFs and MTs interact at the cortical focal plane of plant cells, and that these interactions are altered during coordinated array reorganization. Reassembly experiments suggest dependence of the AF cytoskeleton on the MT cytoskeleton for nucleation of the AFs, which may be facilitated by formins and other factors perhaps analogous to those involved in MT-associated actin nucleation in yeast and animal cells.

## METHODS

### Plant Materials, Growth Conditions, and Genetic Analysis

*Arabidopsis thaliana* Columbia seedlings were surface sterilized, stratified for 3 d, and grown vertically on plates containing Murashige and Skoog media (1× Murashige and Skoog salts, 8 g L<sup>-1</sup> agar, 1× B5 vitamins, and 10.8 g L<sup>-1</sup> sugar) in light (16-h photoperiod) or dark conditions at 21°C for 5 d for light microscopy, and 3 d for confocal microscopy. The FABD:GFP and mCherry:TUA5 constructs were as described in Ketelaar et al. (2004) and Gutierrez et al. (2009), respectively.

### Drug Treatments

Seedlings were immersed in 2 mL of solution with drugs or control solution in 12-well cell culture plates in the dark and were subsequently imaged. Stock solutions of LatB and oryzalin were dissolved in methanol or in DMSO, respectively, and working stocks were made fresh by further dilution in water. For drug washout and recovery experiments, the

seedlings were washed in water three times, after which they were transferred to a fresh solution for recovery.

### Specimen Mounting

The seedlings were mounted between a cover glass and a 1-mm thick 1% agar pad affixed on a circular cover slip, thus stabilizing the sample and preventing it from compression and mechanical damage.

### Microscopy

Light microscopy was performed using a Leica Stereomicroscope (Leica MZ12.5 and Leica DFC420 digital camera). Seedlings expressing GFP:FABD, mCherry:TUA5, and dual-labeled lines of GFP:FABD and mCherry:TUA5 were imaged on a confocal microscope equipped with a CSU-X1 Yokogawa spinning disc head fitted to a Nikon Ti-E inverted microscope, a CFI APO TIRF  $\times 100$  N.A. 1.49 oil immersion objective, an evolve charge-coupled device camera (Photometrics Technology), and a  $\times 1.2$  lens between the spinning disc and camera. GFP was excited at 491 nm and mCherry at 561 nm using a multichannel dichroic and an ET525/50M or an ET595/50M band pass emission filter (Chroma Technology) for GFP and mCherry, respectively. Image acquisitions were performed using Metamorph online premier, version 7.5. Typical exposure times were 600 ms for GFP and 300 ms for mCherry.

### General Image Processing and Analysis

All images were processed using ImageJ software (Rasband, W.S., National Institutes of Health). Background correction was performed using “Subtract Background” tool (rolling ball radius 30–40 pixels), and StackReg (Thévenaz et al., 1998) was used to correct focus drift. Linear adjustments in pixel values were made when measuring signal intensities.

### Rates of Cortical MT Dynamics

$v_g$  and  $v_s$  were measured for the leading ends of single MTs derived from hypocotyls of etiolated seedlings expressing mCherry:TUA5 and treated with jasplakinolide (5  $\mu\text{M}$  for 3 h), or with a mock control. Data were derived from three independent seedlings for control and treated lines, and the number of ends measured for control cells was  $n = 51$  ( $v_s$ ) and 76 ( $v_g$ ), and for jasplakinolide-treated seedlings was  $n = 43$  ( $v_s$ ) and 71 ( $v_g$ ). The Multiple Kymograph plug-in in ImageJ (National Institutes of Health) using a line width of 3 was used to calculate MT velocities in micrometers per minute. Histograms and statistical comparisons were collated in GraphPad Prism-5 and were presented as shrinkage (red), growth (green), and pause (blue).

### Colocalization Analysis of AFs and MTs

Three random kymographs that stretched the entire length of the cell were generated ( $n = 4$  cells). The kymograph (line width 3) generated from the actin channel was first analyzed, and only AF pauses (i.e., AFs appeared static) that occurred for more than 30 s were considered for further analyses. The AF pauses were subsequently mapped over the kymograph from the MT channel to determine colocalization. MT coverage was estimated by using a binary image of the MT channel, which was thresholded, and mean pixel intensity was measured using ImageJ (MTs occupied  $\sim 47\%$  of the area). Statistical estimates of whether the observed colocalization occurred by chance were calculated using a binomial test.

### MT Angles and Fluorescence Intensity of AFs

Three cells each from different seedlings were used for the analysis in all cases. Every 25th image of the time series was taken from a total

of 600 images for the analysis. MT angles were measured with regard to the growth axis and always in a clockwise direction, using the angle tool in ImageJ. AFs were manually thresholded with ImageJ to avoid detection of free GFP:FABD, and histograms were generated to determine the total number of pixels occupied by the thresholded regions, which was then taken as the value for total fluorescence intensity.

### Supplemental Data

The following materials are available in the online version of this article.

**Supplemental Figure 1.** Effect of Cytoskeleton Inhibitors on Seedling Growth and Morphology.

**Supplemental Figure 2.** Light-Induced Changes to AF-MT Coalignment and AF Polymerization at Sites of MT.

**Supplemental Figure 3.** AF-MT Recovery after Drug-Induced Depolymerization.

**Supplemental Movie 1.** Effect of Jasplakinolide on AF Dynamics.

**Supplemental Movie 2.** Actin Fragments Appear over the MTs following 3 h of 5  $\mu\text{M}$  Jasplakinolide Treatment.

**Supplemental Movie 3.** Colocalization of AFs and MTs.

**Supplemental Movie 4.** AF and MT Colocalization Mediated by AF Waving Phenomenon.

**Supplemental Movie 5.** MT Orientation and AF Distribution upon Light Exposure.

**Supplemental Movie 6.** Actin-Related Fragments Appear Adjacent to MTs after 3 h of latB Washout.

**Supplemental Movie 7.** Actin-Related Fragments Move along the MTs 5 h after 1  $\mu\text{M}$  latB Treatment and Washout.

**Supplemental Movie 8.** Movement of Short Actin-Related Structures along the Plus End of MTs 5 h after latB Washout and Actin Recovery.

**Supplemental Movie 9.** Actin Cytoskeleton Recovery 24 h following latB Washout in the Absence of Oryzalin.

**Supplemental Movie 10.** AF Polymerization at Sites Coincident with MTs.

**Supplemental Movie 11.** Actin Cytoskeleton Recovery 6 h following latB Washout in the Presence of 20  $\mu\text{M}$  Oryzalin.

**Supplemental Movie 12.** Actin Cytoskeleton Recovery 24 h following latB Washout in the Presence of 20  $\mu\text{M}$  Oryzalin.

**Supplemental Movie 13.** MT Recovery 6 h following Oryzalin Washout in the Absence of latB.

**Supplemental Movie 14.** MT Recovery 24 h following Oryzalin Washout in the Absence of latB.

**Supplemental Movie 15.** MT Recovery 6 h following Oryzalin Washout in the Presence of 1  $\mu\text{M}$  latB.

**Supplemental Movie 16.** MT Recovery 24 h following Oryzalin Washout in the Presence of 1  $\mu\text{M}$  latB.

**Supplemental Movie 17.** Actin Cytoskeleton and MT Recovery 48 h following Oryzalin and latB Washout.

**Supplemental Movie 18.** Recovery of AFs and MTs following 16 h of 1  $\mu\text{M}$  latB and 20  $\mu\text{M}$  Oryzalin Treatment, with an Additional 6 h of 20  $\mu\text{M}$  Oryzalin Treatment.

**Supplemental Movie 19.** Recovery of AFs and MTs following 16 h of 1  $\mu\text{M}$  latB and 20  $\mu\text{M}$  Oryzalin Treatment, with an Additional 6 h of 1  $\mu\text{M}$  latB Treatment.

## ACKNOWLEDGMENTS

We thank Olivier Hamant and Markus Grebe for the critical comments on the manuscript, Anne Mie C. Emons, Zoran Nikoloski, and Florian Hollandt for stimulating discussion about the topic, and Eugenia Maximova for input on the microscopy at the Max Planck Institute. A.S. and S.P. were financed through the Max Planck Gesellschaft.

## AUTHOR CONTRIBUTIONS

A.S. performed research; A.S., J.J.L., T.K., and S.P. designed the research; R.G. and D.W.E. contributed new material; A.S., J.J.L., and S.D. analyzed the data; and A.S., J.J.L., S.D., R.G., T.K., D.W.E., and S.P. wrote the article.

Received June 2, 2011; revised June 2, 2011; accepted June 6, 2011; published June 21, 2011.

## REFERENCES

- Ambrose, J.C., and Wasteneys, G.O.** (2008). CLASP modulates microtubule-cortex interaction during self-organization of acentrosomal microtubules. *Mol. Biol. Cell* **19**: 4730–4737.
- Barton, D.A., and Overall, R.L.** (2010). Cryofixation rapidly preserves cytoskeletal arrays of leaf epidermal cells revealing microtubule co-alignments between neighbouring cells and adjacent actin and microtubule bundles in the cortex. *J. Microsc.* **237**: 79–88.
- Baskin, T.I., Wilson, J.E., Cork, A., and Williamson, R.E.** (1994). Morphology and microtubule organization in *Arabidopsis* roots exposed to oryzalin or taxol. *Plant Cell Physiol.* **35**: 935–942.
- Basu, R., and Chang, F.** (2007). Shaping the actin cytoskeleton using microtubule tips. *Curr. Opin. Cell Biol.* **19**: 88–94.
- Blancaflor, E.B.** (2000). Cortical actin filaments potentially interact with cortical microtubules in regulating polarity of cell expansion in primary roots of maize (*Zea mays* L.). *J. Plant Growth Regul.* **19**: 406–414.
- Bubb, M.R., Senderowicz, A.M., Sausville, E.A., Duncan, K.L., and Korn, E.D.** (1994). Jasplakinolide, a cytotoxic natural product, induces actin polymerization and competitively inhibits the binding of phalloidin to F-actin. *J. Biol. Chem.* **269**: 14869–14871.
- Chan, J., Calder, G., Fox, S., and Lloyd, C.** (2007). Cortical microtubule arrays undergo rotary movements in *Arabidopsis* hypocotyl epidermal cells. *Nat. Cell Biol.* **9**: 171–175.
- Chan, J., Crowell, E., Eder, M., Calder, G., Bunnewell, S., Findlay, K., Vernhettes, S., Höfte, H., and Lloyd, C.** (2010). The rotation of cellulose synthase trajectories is microtubule dependent and influences the texture of epidermal cell walls in *Arabidopsis* hypocotyls. *J. Cell Sci.* **123**: 3490–3495.
- Chaves, I., Pokorný, R., Byrdin, M., Hoang, N., Ritz, T., Brettel, K., Essen, L.O., van der Horst, G.T., Batschauer, A., and Ahmad, M.** (2011). The cryptochromes: Blue light photoreceptors in plants and animals. *Annu. Rev. Plant Biol.* **62**: 335–364.
- Christie, J.M.** (2007). Phototropin blue-light receptors. *Annu. Rev. Plant Biol.* **58**: 21–45.
- Collings, D.A.** (2008). Crossed wires: Interactions and cross-talk between the microtubule and microfilament networks in plants. In *Plant Cell Monographs: Plant Microtubules, Development, and Flexibility*, P. Nick, ed (Berlin: Springer), pp. 47–82.
- Collings, D.A., and Wasteneys, G.O.** (2005). Actin microfilament and microtubule distribution patterns in the expanding root of *Arabidopsis thaliana*. *Can. J. Bot.* **83**: 579–590.
- Deeks, M.J., Fendrych, M., Smertenko, A., Bell, K.S., Oparka, K., Cvrcková, F., Zársky, V., and Hussey, P.J.** (2010). The plant formin AtFH4 interacts with both actin and microtubules, and contains a newly identified microtubule-binding domain. *J. Cell Sci.* **123**: 1209–1215.
- Dixit, R., and Cyr, R.J.** (2004). Encounters between dynamic cortical microtubules promote ordering of the cortical array through angle-dependent modifications of microtubule behavior. *Plant Cell* **16**: 3274–3284.
- Ehrhardt, D.W., and Shaw, S.L.** (2006). Microtubule dynamics and organization in the plant cortical array. *Annu. Rev. Plant Biol.* **57**: 859–875.
- Fu, Y., Gu, Y., Zheng, Z., Wasteneys, G., and Yang, Z.** (2005). *Arabidopsis* interdigitating cell growth requires two antagonistic pathways with opposing action on cell morphogenesis. *Cell* **120**: 687–700.
- Goode, B.L., Drubin, D.G., and Barnes, G.** (2000). Functional cooperation between the microtubule and actin cytoskeletons. *Curr. Opin. Cell Biol.* **12**: 63–71.
- Gutierrez, R., Lindeboom, J.J., Paredes, A.R., Emons, A.M., and Ehrhardt, D.W.** (2009). *Arabidopsis* cortical microtubules position cellulose synthase delivery to the plasma membrane and interact with cellulose synthase trafficking compartments. *Nat. Cell Biol.* **11**: 797–806.
- Hussey, P.J., Yuan, M., Calder, G., Khan, S., and Lloyd, C.W.** (1998). Microinjection of pollen-specific actin-depolymerizing factor, ZmADF1, reorients F-actin strands in *Tradescantia* stamen hair cells. *Plant J.* **14**: 353–357.
- Ketelaar, T., Allwood, E.G., Anthony, R., Voigt, B., Menzel, D., and Hussey, P.J.** (2004). The actin-interacting protein AIP1 is essential for actin organization and plant development. *Curr. Biol.* **14**: 145–149.
- Kobayashi, H., Fukuda, H., and Shibaoka, H.** (1988). Interrelation between the spatial disposition of actin filaments and microtubules during the differentiation of tracheary elements in cultured *Zinnia* cells. *Protoplasma* **143**: 29–37.
- Li, Y., Shen, Y., Cai, C., Zhong, C., Zhu, L., Yuan, M., and Ren, H.** (2010). The type II *Arabidopsis* formin14 interacts with microtubules and microfilaments to regulate cell division. *Plant Cell* **22**: 2710–2726.
- Mandato, C.A., and Bement, W.M.** (2003). Actomyosin transports microtubules and microtubules control actomyosin recruitment during *Xenopus* oocyte wound healing. *Curr. Biol.* **13**: 1096–1105.
- Martin, S.G., and Chang, F.** (2005). New end take off: Regulating cell polarity during the fission yeast cell cycle. *Cell Cycle* **4**: 1046–1049.
- Morejohn, L.C., Bureau, T., Molé-Bajer, J., Bajer, A.S., and Fosket, D.E.** (1987). Oryzalin, a dinitroaniline herbicide, binds to plant tubulin and inhibits microtubule polymerization *in vitro*. *Planta* **172**: 252–264.
- Murata, T., Sonobe, S., Baskin, T.I., Hyodo, S., Hasezawa, S., Nagata, T., Horio, T., and Hasebe, M.** (2005). Microtubule-dependent microtubule nucleation based on recruitment of  $\gamma$ -tubulin in higher plants. *Nat. Cell Biol.* **7**: 961–968.
- Nakamura, M., Ehrhardt, D.W., and Hashimoto, T.** (2010). Microtubule and katanin-dependent dynamics of microtubule nucleation complexes in the acentrosomal *Arabidopsis* cortical array. *Nat. Cell Biol.* **12**: 1064–1070.
- Paredes, A.R., Somerville, C.R., and Ehrhardt, D.W.** (2006). Visualization of cellulose synthase demonstrates functional association with microtubules. *Science* **312**: 1491–1495.
- Petrásek, J., and Schwarzerová, K.** (2009). Actin and microtubule cytoskeleton interactions. *Curr. Opin. Plant Biol.* **12**: 728–734.
- Pouter, N.S., Vatovec, S., and Franklin-Tong, V.E.** (2008). Microtubules are a target for self-incompatibility signaling in *Papaver* pollen. *Plant Physiol.* **146**: 1358–1367.
- Preuss, M.L., Kovar, D.R., Lee, Y.-R.J., Staiger, C.J., Delmer, D.P., and Liu, B.** (2004). A plant-specific kinesin binds to actin microfilaments and interacts with cortical microtubules in cotton fibers. *Plant Physiol.* **136**: 3945–3955.

- Saedler, R., Mathur, N., Srinivas, B.P., Kernebeck, B., Hülkamp, M., and Mathur, J.** (2004). Actin control over microtubules suggested by DISTORTED2 encoding the *Arabidopsis* ARPC2 subunit homolog. *Plant Cell Physiol.* **45**: 813–822.
- Salmon, W.C., Adams, M.C., and Waterman-Storer, C.M.** (2002). Dual-wavelength fluorescent speckle microscopy reveals coupling of microtubule and actin movements in migrating cells. *J. Cell Biol.* **158**: 31–37.
- Shaw, S.L., Kamyar, R., and Ehrhardt, D.W.** (2003). Sustained microtubule treadmilling in *Arabidopsis* cortical arrays. *Science* **300**: 1715–1718.
- Sheahan, M.B., Staiger, C.J., Rose, R.J., and McCurdy, D.W.** (2004). A green fluorescent protein fusion to actin-binding domain 2 of *Arabidopsis* fimbrin highlights new features of a dynamic actin cytoskeleton in live plant cells. *Plant Physiol.* **136**: 3968–3978.
- Staiger, C.J., Sheahan, M.B., Khurana, P., Wang, X., McCurdy, D.W., and Blanchoin, L.** (2009). Actin filament dynamics are dominated by rapid growth and severing activity in the *Arabidopsis* cortical array. *J. Cell Biol.* **184**: 269–280.
- Strachen, S.D., and Hess, F.D.** (1983). The biochemical mechanism of action of the dinitroaniline herbicide oryzalin. *Pestic. Biochem. Physiol.* **20**: 141–150.
- Suetsugu, N., Yamada, N., Kagawa, T., Yonekura, H., Uyeda, T.Q.P., Kadota, A., and Wada, M.** (2010). Two kinesin-like proteins mediate actin-based chloroplast movement in *Arabidopsis thaliana*. *Proc. Natl. Acad. Sci. USA* **107**: 8860–8865.
- Szymanski, D.B.** (2009). Plant cells taking shape: New insights into cytoplasmic control. *Curr. Opin. Plant Biol.* **12**: 735–744.
- Takesue, K., and Shibaoka, H.** (1998). The cyclic reorientation of cortical microtubules in epidermal cells of azuki bean epicotyls: The role of actin filaments in the progression of the cycle. *Planta* **205**: 539–546.
- Thévenaz, P., Ruttimann, U.E., and Unser, M.** (1998). A pyramid approach to subpixel registration based on intensity. *IEEE Trans. Image Process.* **7**: 27–41.
- Timmers, A.C.J., Valloton, P., Heym, C., and Menzel, D.** (2007). Microtubule dynamics in root hairs of *Medicago truncatula*. *Eur. J. Cell Biol.* **86**: 69–83.
- Tominaga, M., Yokota, E., Vidali, L., Sonobe, S., Hepler, P.K., and Shimmen, T.** (2000). The role of plant villin in the organization of the actin cytoskeleton, cytoplasmic streaming and the architecture of the transvacuolar strand in root hair cells of *Hydrocharis*. *Planta* **210**: 836–843.
- Traas, J.A., Doonan, J.H., Rawlins, D.J., Shaw, P.J., Watts, J., and Lloyd, C.W.** (1987). An actin network is present in the cytoplasm throughout the cell cycle of carrot cells and associates with the dividing nucleus. *J. Cell Biol.* **105**: 387–395.
- Ueda, K., and Matsuyama, T.** (2000). Rearrangement of cortical microtubules from transverse to oblique or longitudinal in living cells of transgenic *Arabidopsis thaliana*. *Protoplasma* **213**: 28–38.
- Wen, Y., Eng, C.H., Schmoranzler, J., Cabrera-Poch, N., Morris, E.J., Chen, M., Wallar, B.J., Alberts, A.S., and Gundersen, G.G.** (2004). EB1 and APC bind to mDia to stabilize microtubules downstream of Rho and promote cell migration. *Nat. Cell Biol.* **6**: 820–830.
- Whippo, C.W., Khurana, P., Davis, P.A., DeBlasio, S.L., DeSloover, D., Staiger, C.J., and Hangarter, R.P.** (2011). THRUMIN1 is a light-regulated actin-bundling protein involved in chloroplast motility. *Curr. Biol.* **21**: 59–64.
- Xu, T., Qu, Z., Yang, X., Qin, X., Xiong, J., Wang, Y., Ren, D., and Liu, G.** (2009). A cotton kinesin GhKCH2 interacts with both microtubules and microfilaments. *Biochem. J.* **421**: 171–180.

**Live Cell Imaging Reveals Structural Associations between the Actin and Microtubule  
Cytoskeleton in *Arabidopsis***

Arun Sampathkumar, Jelmer J. Lindeboom, Seth Debolt, Ryan Gutierrez, David W. Ehrhardt, Tijs  
Ketelaar and Staffan Persson

*Plant Cell* 2011;23;2302-2313; originally published online June 21, 2011;

DOI 10.1105/tpc.111.087940

This information is current as of February 1, 2012

<b>Supplemental Data</b>	<a href="http://www.plantcell.org/content/suppl/2011/06/08/tpc.111.087940.DC1.html">http://www.plantcell.org/content/suppl/2011/06/08/tpc.111.087940.DC1.html</a> <a href="http://www.plantcell.org/content/suppl/2011/06/13/tpc.111.087940.DC2.html">http://www.plantcell.org/content/suppl/2011/06/13/tpc.111.087940.DC2.html</a>
<b>References</b>	This article cites 47 articles, 15 of which can be accessed free at: <a href="http://www.plantcell.org/content/23/6/2302.full.html#ref-list-1">http://www.plantcell.org/content/23/6/2302.full.html#ref-list-1</a>
<b>Permissions</b>	<a href="https://www.copyright.com/ccc/openurl.do?sid=pd_hw1532298X&amp;issn=1532298X&amp;WT.mc_id=pd_hw1532298X">https://www.copyright.com/ccc/openurl.do?sid=pd_hw1532298X&amp;issn=1532298X&amp;WT.mc_id=pd_hw1532298X</a>
<b>eTOCs</b>	Sign up for eTOCs at: <a href="http://www.plantcell.org/cgi/alerts/ctmain">http://www.plantcell.org/cgi/alerts/ctmain</a>
<b>CiteTrack Alerts</b>	Sign up for CiteTrack Alerts at: <a href="http://www.plantcell.org/cgi/alerts/ctmain">http://www.plantcell.org/cgi/alerts/ctmain</a>
<b>Subscription Information</b>	Subscription Information for <i>The Plant Cell</i> and <i>Plant Physiology</i> is available at: <a href="http://www.aspb.org/publications/subscriptions.cfm">http://www.aspb.org/publications/subscriptions.cfm</a>